Anal. Bioanal. Electrochem., Vol. 15, No. 8, 2023, 668-695
https://www.doi.org/10.22034/abec.2023.707326

Analytical & Bioanalytical Electrochemistry

Review

Nanocomposite based Electrochemical Sensors for Determination of Some Biologically Important Compounds: A Review

Vinod Kumar Vashistha,[1,*] Renu Bala,[2] Ankit Mittal,[1] Dipak Kumar Das,[1,*] Shubham Sharma,[3] and Rajasekhar VSR Pullabhotla[4]

[1]*Department of Chemistry, GLA University, Mathura, 281406, India*
[2]*Department of Chemistry, Kalindi College, University of Delhi, Delhi, India*
[3]*Department of ASHD, G B Pant Institute of Engineering and Technology, Pauri Garhwal, Uttarakhand, India*
[4]*Department of Chemistry, Faculty of Science, Agriculture and Engineering, University of Zululand, P/Bag X1001, KwaDlangezwa, 3886, South Africa*

*Corresponding Author, Tel.: +91-5662 250 900
E-Mails: vinod.vashistha@gla.ac.in ; deepak.das@gla.ac.in

Received: 27 May 2023 / Accepted with minor revision: 23 August 2023 / Published online: 31 August 2023

Abstract- Electrochemical methods have become increasingly popular in the pharmaceutical and drug analysis sectors due to their numerous benefits, such as high sensitivity, selectivity, and specificity. Electrochemical-based nanomaterials are adjustable and can be influenced by the type of electrode used and the applied potential. Electroanalytical methods have proven to be a useful analytical technology that has seen increased utility in the pharmaceutical business in recent years. In the last five years, there have been significant developments in the synthesis and use of novel electrochemical sensors in drug analysis. These developments have been driven by advancements in instrumentation and an increased understanding of electrochemical methods. This review concludes the current state-of-the-art in electrochemical sensors for pharmaceutical analysis and future perspectives in this field. We highlight the need for more standardized methods for the determination of biologically important compounds such as dopamine, guanine, adenine, and uric acid using electrochemical sensors and the development of multiplexed sensors for simultaneous analysis of multiple drugs.

Keywords- Electrochemical nanosensors; Drug analysis; Cyclic voltammetry; Biochemicals; Nanocomposites

1. INTRODUCTION

Pharmaceutical analysis is a crucial aspect of the drug development process that involves the evaluation of the physicochemical, biological, and microbiological properties of drug molecules to ensure their safety, efficacy, and quality [1-3]. Common analytical techniques used for the detection and quantification of clinically important pharmaceuticals include mass spectrometry [4,5], high-performance liquid chromatography (HPLC) [6-9], fluorescence spectroscopy [10,11], ion-pairing liquid chromatography [12-14], micellar electrokinetic chromatography [15-17], and capillary zone electrophoresis [18,19]. These analytical techniques are important tools in the development and testing of pharmaceuticals, and they play a crucial role in ensuring the safety and efficacy of drugs for clinical use. In addition, electrochemical methods are commonly used in pharmaceutical analysis for the detection, quantification, and characterization of drugs and their metabolites [20,21]. These methods rely on the use of electrodes to measure the electrical properties of analytes in solution.

Electroanalytical nanosensors are widely used in various fields because of their high adaptability and sensitivity. These sensors are capable of detecting and measuring very small amounts of biomolecules or other chemical analytes in a sample, making them useful in a range of applications from medical diagnostics to environmental monitoring [20]. Biomolecules and their metabolic by-products have specific electronic structures that can be detected by electroanalytical sensors. These sensors work by measuring changes in electrical properties such as voltage or current when the target molecules interact with the sensor surface. These changes can then be converted into analytical signals that can be used to quantify the amount of the target molecule in the sample [22]. Because of their high sensitivity and selectivity, electroanalytical sensors are often used in biomedical research and diagnostics. For example, they can be used to detect biomarkers of disease or to monitor drug levels in patients. In addition, electroanalytical sensors are used in food and drug industries to monitor the quality and safety of products.

Electrochemical sensors have their own set of challenges, such as high overpotential, slow transfer of electrons, poor reproducibility, and fouling by oxidation product accumulation [23]. However, they are still considered the device of choice for many applications due to their cost-effective production, quick processing rates, and data collection ability, as well as their ability to operate in complex, concentrated biological samples.

Nanosized oxides possess unique physical and chemical properties, such as a high surface area to volume ratio, which enhances their electrochemical properties. The availability of more reaction sites due to their large surface area and lattice defects, in addition to low overpotential, leads to excellent electrochemical conductivity, making them suitable for various applications, including as sensor modifiers [24]. Furthermore, nanosized oxides are stable and durable, making them ideal electrode materials. They are also easily prepared and cost-effective, which is crucial for large-scale production. These features make nanosized oxides a promising

material for many electrochemical applications, including batteries, supercapacitors, sensors, and catalysts. Overall, the resurgence in interest in electrochemical methods in the investigation of medications and pharmaceuticals can be attributed to the development of more advanced instrumentation, as well as a greater understanding of the capabilities and limitations of these techniques. As researchers continue to refine and improve electrochemical methods, these techniques are likely to become even more widely used in pharmaceutical research and development.

One of the key advantages of electrochemical sensors is their ability to detect minute quantities of analytes without causing significant damage or altering the sample. This is particularly important in medical diagnostics, where the accuracy and precision of the test results are crucial. In the years to come, electrochemical sensors are expected to play an increasingly important role in medical diagnostics, as they offer several advantages over traditional diagnostic methods, such as faster results, lower costs, and greater accuracy [25]. With further advancements in sensing technology, biosensors will likely become even more sensitive, specific, and versatile, paving the way for new applications in healthcare and beyond.

1.1. Scope of the review

In this review, we discuss the recent developments in the field of nanocomposite-based electrochemical sensors for biologically important compounds such as dopamine, guanine, adenine, and uric acid, etc. The review highlights the different types of nanocomposites used in sensor fabrication, including metal and metal oxide nanoparticles, graphene, and graphite powder. We also discuss the various approaches used to modify the nanocomposite surfaces for enhancing sensor performance, such as functionalization with specific molecules. Moreover, the review highlights the key advantages of nanocomposite-based electrochemical sensors, such as their ability to detect biologically important compounds at low concentrations, high selectivity, and real-time monitoring. The review covers the recent advances in the fabrication of nanocomposite-based electrochemical sensors for the detection of various biologically important compounds, including dopamine, guanine, adenine, and uric acid. This review concludes with a summary of the state-of-the-art in electrochemical nanosensors for pharmaceutical analysis and future perspectives in this field.

2. ELECTROCHEMICAL METHODS

Electrochemical methods refer to a group of techniques that utilize the principles of electrochemistry to study and manipulate chemical reactions and processes. These methods involve the application of an electrical potential or current to a chemical system, allowing for the measurement and control of various electrochemical parameters [26]. Some commonly used electrochemical methods:

2.1. Potentiometry

Potentiometry is a widely used analytical technique in electrochemistry. It involves measuring the potential difference, also known as the electromotive force (EMF), between two electrodes in an electrochemical cell. The electrodes are usually made of an inert material, such as platinum, and are immersed in the solution being analyzed. In potentiometry, the potential difference is measured without any current flow between the electrodes. The measured potential is a direct result of the concentration of the analyte or ions of interest in the solution [27]. The potential difference is typically measured using a voltmeter or a pH meter, depending on the specific application. The key principle behind potentiometry is that the potential difference across the electrodes is proportional to the logarithm of the concentration of the analyte. This relationship is described by the Nernst equation, which relates the measured potential to the analyte concentration and other factors, such as temperature and electrode potential. The measurement process involves constructing a reference electrode and a working electrode. The reference electrode provides a stable and known potential against which the potential of the working electrode can be measured. The working electrode, which is in contact with the solution being analyzed, responds to changes in the analyte concentration and generates a potential difference. Potentiometry finds applications in various fields, including chemical analysis, environmental monitoring, pharmaceuticals, and biomedical research. It is commonly used for the determination of pH, as well as the quantification of various ions, such as chloride, sodium, calcium, and heavy metal ions. By measuring the potential difference and comparing it to calibration curves or standard solutions, the concentration of the analyte can be determined.

2.2. Voltammetry

Voltammetry is an electrochemical technique that involves applying a potential sweep or step to an electrochemical cell and measuring the resulting current. It is widely used for qualitative and quantitative analysis of analytes in a solution, as well as for studying electrochemical reactions. In voltammetry, a potential is applied to the working electrode, while the current response is measured as a function of the applied potential [28]. The working electrode is typically made of a material that is electrochemically active and specific to the analyte of interest. Common materials include platinum, gold, glassy carbon, and other conductive materials. The potential is varied either by sweeping the potential linearly with time (linear sweep voltammetry) or by stepping the potential in discrete increments (cyclic voltammetry or square wave voltammetry). The resulting current is measured, and the information obtained from the current-potential relationship is used to analyze the electrochemical system.

Voltammetry can provide valuable information about the redox behavior of species in a solution. It can be used to determine the concentration of an analyte by generating a calibration

curve relating the current response to known concentrations. This makes it a useful quantitative analytical technique. Additionally, voltammetry is often employed to study the kinetics and mechanisms of electrochemical reactions. By examining the shape of the voltammogram (the plot of current vs. potential), important parameters such as the peak potential, peak current, and peak width can be obtained, providing insights into the underlying chemical and electrochemical processes. Different variants of voltammetry, such as differential pulse voltammetry, stripping voltammetry, and rotating disk electrode voltammetry, offer specific advantages and are used for various applications. These techniques can provide enhanced sensitivity, selectivity, and information about specific analytes or processes. Voltammetry is a versatile electrochemical technique that is widely utilized for both qualitative and quantitative analysis, as well as the investigation of electrochemical reactions. It offers valuable insights into the behavior of analytes in solution and has applications in fields such as environmental monitoring, pharmaceutical analysis, and electrochemical sensor development.

2.3. Cyclic Voltammetry

Cyclic voltammetry is an electrochemical technique that involves sweeping the applied potential linearly in one direction and then reversing the direction to return to the initial potential. It is widely used to study the redox behavior, kinetics, and thermodynamics of electroactive species in a solution [29]. In cyclic voltammetry, the potential is scanned at a constant rate, typically referred to as the scan rate. The potential is swept from a starting potential to a desired maximum potential in one direction, known as the forward scan. Then, the potential is reversed and swept back to the starting potential, which is known as the reverse scan. The resulting current is measured as a function of the applied potential. The technique offers several advantages, such as simplicity, rapid data acquisition, and the ability to provide information about multiple electrochemical parameters in a single experiment. However, it is important to note that the interpretation of cyclic voltammetry data requires careful consideration of experimental conditions, electrode properties, and underlying reaction mechanisms.

2.4. Amperometry

Amperometry is an electrochemical technique that measures the current flowing through an electrochemical cell at a constant applied potential. It is commonly used for detecting and quantifying analytes that undergo electrochemical reactions. In amperometry, a constant potential is applied to the working electrode, and the resulting current is measured. The working electrode is typically made of a material that is specific to the electrochemical reaction of interest [30]. For example, in blood glucose sensors, the working electrode is often made of glucose oxidase, which catalyzes the oxidation of glucose. When the analyte of interest is

present in the solution, it undergoes an electrochemical reaction at the working electrode surface, leading to a change in the current. The magnitude of the current is directly proportional to the concentration of the analyte in the solution.

Amperometry offers several advantages for analytical applications, including high sensitivity, rapid response, and the ability to detect and quantify analytes in real time. It is commonly used in various fields, such as clinical diagnostics, environmental monitoring, and food analysis. In the case of blood glucose sensors, amperometry is widely employed for monitoring blood glucose levels in individuals with diabetes. The sensor detects the glucose in a blood sample by measuring the current resulting from the oxidation of glucose at the working electrode. By calibrating the sensor using known glucose concentrations, the current response can be correlated with the glucose concentration in the blood. It's important to note that amperometry requires careful calibration and consideration of potential interferences to ensure accurate and reliable measurements. Factors such as electrode fouling, background current, and interfering substances can affect the performance of amperometric measurements. However, with proper experimental design and calibration, amperometry can be a valuable tool for the detection and quantification of electroactive analytes.

2.5. Impedance Spectroscopy

Impedance spectroscopy is an electrochemical technique that measures the electrical impedance of a system as a function of frequency. It provides valuable information about the resistive and capacitive properties of electrochemical systems and is widely used for the characterization of electrochemical interfaces and materials. By analyzing the impedance as a function of frequency, impedance spectroscopy enables the investigation of various electrochemical processes occurring within a system. In impedance spectroscopy, a small sinusoidal signal is applied to the system across a range of frequencies [31]. The resulting current response is then measured, and the ratio of the applied voltage to the measured current is determined, giving the complex impedance.

Impedance spectroscopy is widely applied in various fields, including electrochemistry, materials science, energy storage, corrosion analysis, and biosensing. It is particularly useful in the development and optimization of electrochemical devices and systems, as it provides valuable information on their performance, stability, and efficiency. However, it is important to note that interpreting impedance spectra can be complex, as the impedance response is influenced by multiple factors and often requires mathematical modeling and analysis techniques such as equivalent circuit modeling and data fitting. Additionally, impedance spectroscopy is sensitive to experimental conditions, such as electrode preparation, temperature, and solution composition, which need to be carefully controlled and considered during measurements and data interpretation.

2.6. Chronoamperometry and Chronopotentiometry

Chronoamperometry and chronopotentiometry are electrochemical techniques commonly used in the field of electrochemistry to investigate reaction kinetics, electrode processes, and mass transport phenomena [32]. Chronoamperometry involves applying a constant potential to an electrochemical cell and measuring the resulting current as a function of time. This technique is useful for studying the kinetics of electrochemical reactions, including electron transfer processes at the electrode surface. By monitoring the current response over time, information about reaction rates, reaction mechanisms, and diffusion processes can be obtained. During chronoamperometry, the potential is abruptly changed to a desired value, and then the resulting current is recorded over a specific period. The recorded current can be used to calculate parameters such as the rate constant, charge transfer coefficient, and diffusion coefficients.

Chronopotentiometry, on the other hand, involves applying a constant current to an electrochemical cell and measuring the resulting potential as a function of time. This technique is particularly useful for investigating mass transport phenomena and the behavior of redox couples at electrode surfaces. In chronopotentiometry, a constant current is applied, and the potential is recorded over time. The potential changes observed during the experiment can provide information about processes such as diffusion, adsorption/desorption, and electrode kinetics. Both chronoamperometry and chronopotentiometry can be used to study a wide range of electrochemical systems, including batteries, fuel cells, corrosion processes, and electroanalytical methods. These techniques offer valuable insights into the behavior of electrochemical systems under different experimental conditions and can be used to optimize and design electrochemical devices and processes.

2.7. Electrochemical Impedance Spectroscopy (EIS)

EIS is a powerful technique used to measure the impedance of an electrochemical system as a function of frequency. It provides valuable information about the electrical and electrochemical properties of interfaces, making it widely employed for characterizing corrosion processes, fuel cells, batteries, sensors, and various other electrochemical devices. In EIS, a small amplitude alternating current (AC) signal is applied to the electrochemical system across a range of frequencies, typically spanning several orders of magnitude. The resulting current response and potential across the system are measured. By analyzing the relationship between the applied voltage and the resulting current, the impedance of the system can be determined [33]. EIS is a non-destructive technique that provides valuable information about the behavior and performance of electrochemical systems under different operating conditions. It is widely used for research, development, and optimization of electrochemical devices, as well as for monitoring and diagnosing corrosion processes and other electrochemical phenomena.

3. SYNTHESIS OF NANOCOMPOSITE

The combustion technique is a popular method for the synthesis of nanocomposites. This technique involves the exothermic reaction between a fuel and an oxidizer to generate a high-temperature flame or combustion front [34]. The heat and reactive species produced during combustion are utilized to initiate and drive the synthesis of nanocomposite materials.

A general overview of the combustion technique for the synthesis of nanocomposites [35] (Figure 1) is as follows: (i) Selection of fuel and oxidizer: The choice of fuel and oxidizer depends on the specific materials desired for the nanocomposite. Common fuel sources include organic compounds such as sugars, alcohols, or urea, while oxidizers can be nitrates, perchlorates, or metal salts. (ii) Mixing of reactants: The fuel and oxidizer are intimately mixed together in the desired stoichiometric ratio. Other components such as metal precursors, nanoparticles, or additives may also be incorporated into the mixture to achieve the desired composition and properties of the nanocomposite. (iii) Ignition and combustion: The mixture is ignited, typically by applying heat or a spark. The combustion reaction propagates through the mixture, releasing a large amount of energy in the form of heat and light. The high temperatures and reactive species generated during combustion provide the necessary conditions for rapid synthesis. (iv) Nanoparticle formation and growth: The combustion process rapidly heats the mixture, leading to the formation of intermediate species, such as metal oxides or carbides, depending on the composition. These species subsequently undergo nucleation and growth, resulting in the formation of nanoparticles or nanocrystals. (v) Nanocomposite formation: During the combustion process, the nanocrystals or nanoparticles are dispersed within the matrix formed by the combustion products. This results in the formation of a nanocomposite material where the nanoparticles are uniformly distributed within a matrix phase. (vi) Quenching and post-treatment: To prevent further growth or agglomeration of the nanoparticles, the reaction is quenched by cooling the system rapidly. Subsequent post-treatment steps like washing, filtration, and annealing may be performed to remove unwanted by-products or enhance the properties of the nanocomposite.

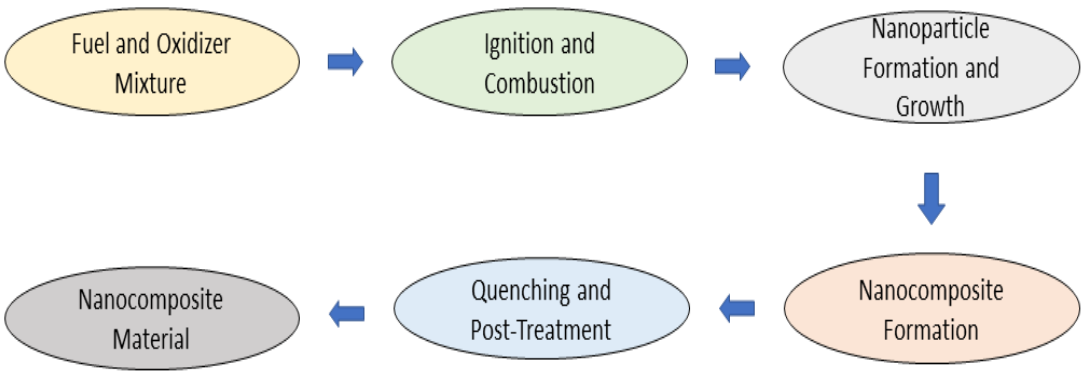

Figure 1. General scheme for the synthesis of nanocomposite using combustion technique

The combustion synthesis technique offers several advantages for nanocomposite synthesis, including simplicity, scalability, and relatively low cost. It allows for the synthesis of a wide range of nanocomposite materials with controlled compositions, particle sizes, and distributions. However, it is important to carefully optimize the process parameters, such as reactant ratios, heating rates, and combustion atmosphere, to ensure the desired properties of the nanocomposite are achieved.

Few examples of synthesis of nanocomposite are described herein in this section. For example, Pramanik et al. reported [36] the synthesis of $NiMn_2O_4$ NPs using a combustion technique, as shown in Figure 2. Briefly, a one-pot synthesis procedure was employed to produce nanoparticles (NPs) of $NiMn_2O_4$. In a 1000-mL beaker, 100 mL of double-distilled water was taken and mixed with 1 g of nickel nitrate, 1.19 g of manganese acetate anhydrous, 5.6 g of mono-ethanolamine, and 23 g of sucrose. To ensure homogeneity, 15 mL of concentrated nitric acid was added to the solution. The mixture was then heated on a hot plate at 150-160^oC until a black fluffy mass was formed. Subsequently, the black fluffy mass was ground using a mortar and pestle. The resulting material was subjected to calcination in a muffle furnace at 600^oC for 6-7 hours, yielding the $NiMn_2O_4$ NPs. The fabrication of an electrochemical sensor based on nickel manganate nanoparticles ($NiMn_2O_4$ NPs) was carried by using a mixture containing $NiMn_2O_4$-NPs and graphite in a ratio of 1:4 (w/w) was prepared by mechanically mixing them in a mortar and pestle. A few drops of paraffin oil were added during the mixing process. An electrode was constructed using a capillary glass tube with an inner diameter of 2 mm and an outer diameter of 5 mm.

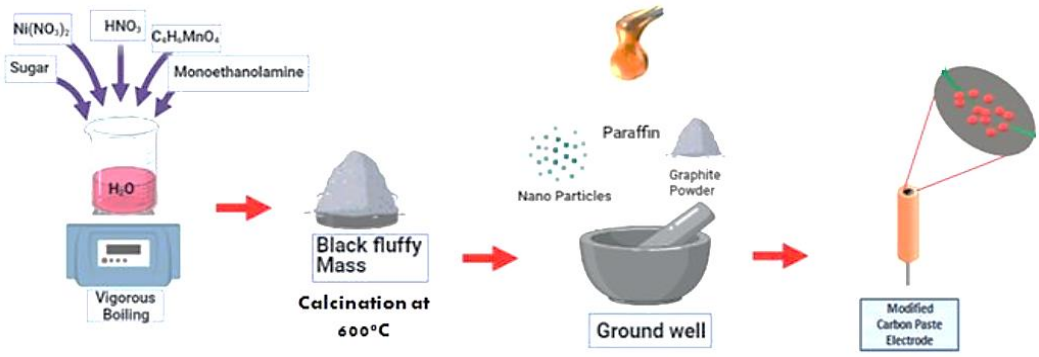

Figure 2. The synthesis of $NiMn_2O_4$ NPs using a combustion technique [36]

The tube was filled with the aforementioned mixture and tightly compressed using a thin metallic rod. To facilitate current conductivity, a platinum wire was inserted at the opposite end of the capillary tube. The same procedure was followed to create bare graphite paste (GP) electrodes. The composite surface was polished using a slurry of Al_2O_3 (0.6 mM). After being washed with ethanol, the electrodes were dried under a nitrogen (N_2) atmosphere until they were completely dry.

Kumar and co-workers used the combustion method for synthesizing $MnFe_2O_4$ NPs [37]. To create a homogeneous solution, manganese acetate (0.01 mol), ferric nitrate (0.02 mol), and sucrose (0.17 mol) were individually dissolved in 100 ml of distilled water. These solutions were then combined in a 1000-mL beaker. After thorough mixing, monoethanolamine (0.25 mol) was added, followed by the addition of nitric acid (0.44 mol) while continuously stirring the mixture. The solution was heated on a hot plate, resulting in the formation of a blackish-fluffy mass due to spontaneous combustion. The obtained blackish mass was subsequently heated in a furnace at 600 °C for 6-7 hours to obtain nanoparticles of $MnFe_2O_4$ (Figure 3).

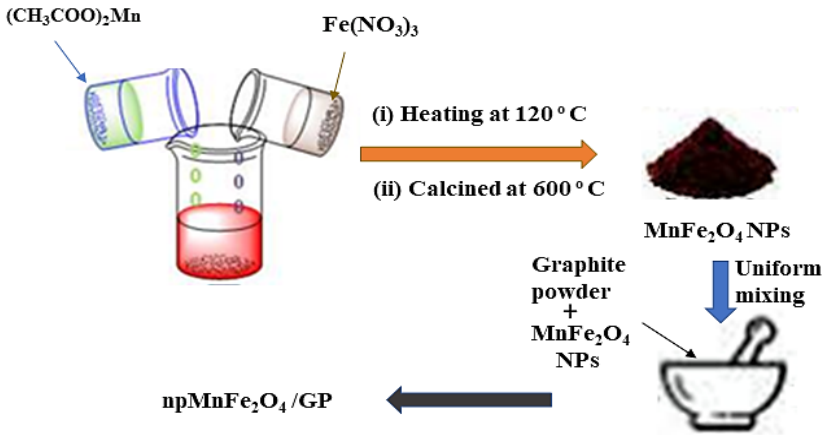

Figure 3. The synthesis of $MnFe_2O_4$ NPs and $MnFe_2O_4$ NPs/GP using a combustion technique [36]

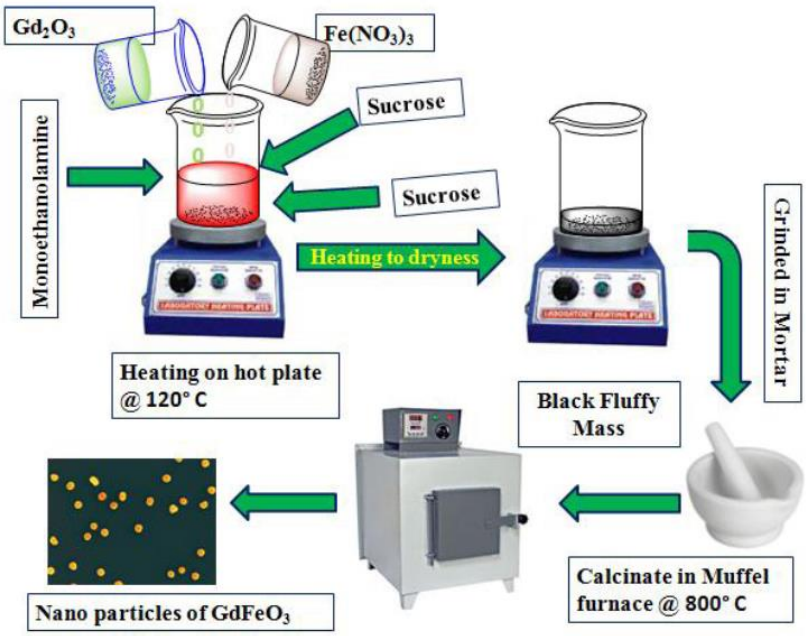

Figure 4. The schematic diagram for the synthesis of $GdFeO_3$ NPs [38]

The study conducted by Pramanik et al. involved the synthesis of gadolinium ferrate NPs ($GdFeO_3$ NPs) [38]. To synthesize gadolinium ferrite nanoparticles ($GdFeO_3$ NPs), gadolinium oxide (1.0 mM) was placed in a 50-mL beaker containing double-distilled water. Nitric acid (3.5 mM) was added to the beaker, and the mixture was heated until a clear solution of gadolinium nitrate was obtained. Next, ferric nitrate (1.0 mM), ethanolamine (1.7 mM), and a sucrose solution (2.5 mM) were added to the beaker, and the mixture was heated on a hot plate at 150 °C until it dried, resulting in the formation of a blackish fluffy mass. After grinding, the brown powder was calcined in a muffle furnace at 800°C for 6 hours to obtain $GdFeO_3$ nanoparticles. Figure 4 provides a schematic representation of the synthesis process for gadolinium ortho ferrite nanoparticles.

3. ELECTROCHEMICAL DETECTIONS OF PHARMACEUTICALS USING NANOSENSORS

Pramanik et al. reported the development of an electrochemical sensor based on nickel manganate nanoparticles ($NiMn_2O_4$ NPs) mixed with graphite paste (GP) for the simultaneous detection of guanine (GU) and uric acid (UA) in a single sample [36]. The sensor showed excellent sensitivity and selectivity towards GU and UA, with a linear response range of 0.1–500 μM for GU and 0.01–100 μM for UA, respectively. The sensor was also found to be stable and reproducible over multiple cycles of measurements.

The electrochemical evaluation showed that $NiMn_2O_4$ NPs/GP exhibited superior electrocatalytic activity compared to GP electrodes with a current value of 108 μA and 87 μA for $NiMn_2O_4$-NPs/GP and GP electrodes, respectively, using $[Fe(CN)_6]^{4-}/[Fe(CN)_6]^{3-}$ as a standard redox system. CV analysis of $NiMn_2O_4$ NPs/GP for UA and GU showed peak current values of 383 mV at 9.31 μA and 978 mV at 10.74 μA, respectively, while the peak current value for GP electrode alone was 6.05 μA for UA and 5.45 μA for GU. The CV analysis also showed (Figure 5a-5c) two distinct peaks for UA and GU with a separation of 434 mV, indicating good separation and excellent electrocatalytic performance for detection and faster electron transfer. DPV plots (Figure 5d) revealed a detection limit of 400 nm for both UA and GU, with a range of 3 to 120 μM for UA and 0.5 to 100 μM for GU. The scan rate for CV analysis was fixed at 100 mVs^{-1}, while for DPV plots, the scan rate was kept at 50 mVs^{-1}. Overall, the results indicate the potential of $NiMn_2O_4$-NPs/GP electrodes for the sensitive and selective detection of UA and GU.

The linear ranges reported indicate the concentration range over which the sensor response is proportional to the concentration of the analyte, and they differ between UA and GU. For UA, the linear range is 1.0 to 120 M, whereas for GU, it is 0.5 to 100 mM. The detection limits of the sensor for UA and GU were reported to be 400 and 400 nM, respectively. In the DPV approach, the fixed GU concentration was kept at 100 μM while the variable UA concentration

ranged from 3-120 µM. The linear range for the detection of UA was found to be between 1 and 40 µM.

The combination of $NiMn_2O_4$ NPs and GP allowed for improved electron transfer and enhanced electrocatalytic activity, leading to improved sensing performance. The use of this sensor could have important implications for the detection of GU and UA in biological samples, as these compounds are relevant biomarkers for several diseases, including gout and kidney disorders. Overall, this study highlights the potential of using nanomaterials and electrochemical sensing for the development of highly sensitive and selective diagnostic tools.

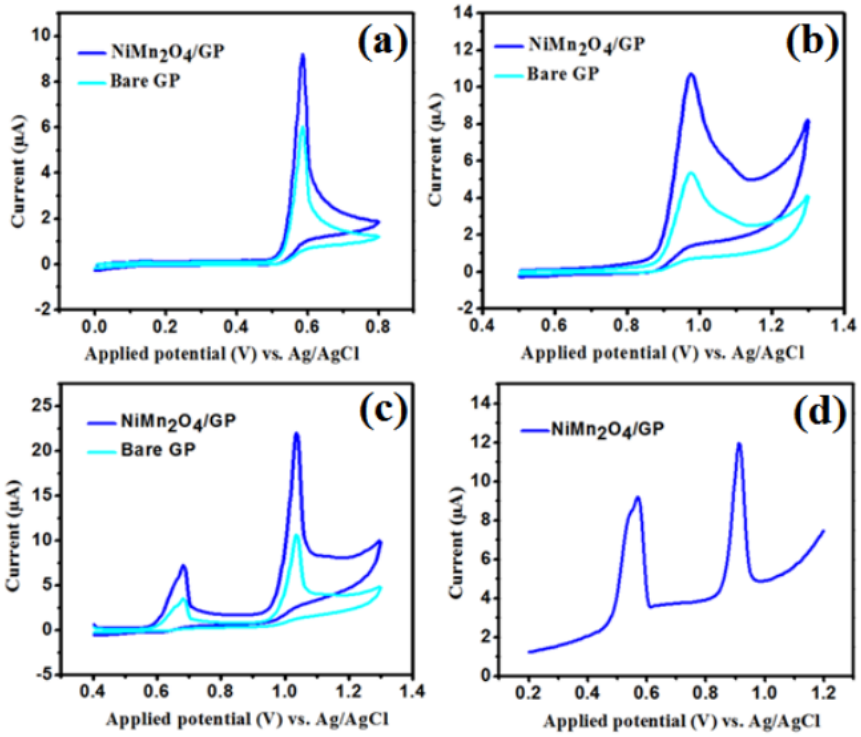

Figure 5. CV plots of (a) 0.1 mM of UA; (b) 0.1 mM of GU; (c) 0.1 mM UA and 0.1 mM GU in combination; (d) DPV plot of 0.1 mM UA and 0.1 mM GU in combination [Background electrolyte: 0.1 M phosphate (pH 5.0); scan rate of CV: 100 mVs^{-1}; scan-rate of DPV:50 mVs^{-1}. Adapted with permission from ref. [36] Copyright @ authors

Kumar et al. conducted a study where they synthesized $MnFe_2O_4$ NPs using a combustion process and characterized the NPs using XRD, TGA, and FESEM techniques [37]. The combustion protocol was used for the synthesis of $MnFe_2O_4$ NPs, and the fabrication of the graphite powder electrode modified with $MnFe_2O_4$ NPs. This method of synthesis and electrode fabrication can have potential applications in the field of energy storage and sensing technology. They also prepared a working electrode for electrochemical analysis using CV by mixing graphite powder with the NPs (Figure 6). The effect of pH on the performance of newly developed sensors was investigated. The data in Figure 6c suggests that the highest peak current value was obtained at pH 6.0. The working electrode used in the study was created using

$MnFe_2O_4$ NPs/GP, which is a newly synthesized nanomaterial. The electrode exhibited oxidation potential at 376 mV and reduction potential at 185 mV, with corresponding oxidation and reduction currents of 44.9 A and 32.16 A, respectively (Figure 6c). Overall, the oxidation and reduction potentials and currents reported suggest that the working electrode may have potential applications in various electrochemical sensing and detection systems. The results showed that $MnFe_2O_4$ NPs could be used as a cathode for long-term charge and discharge processing in lithium-ion batteries, as well as a sensor.

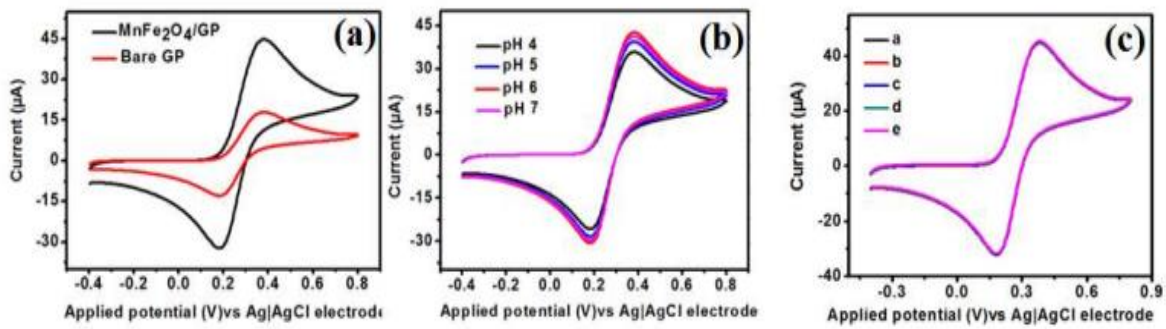

Figure 6. (a) Cyclic voltammogram in standard redox system using $K_3[Fe(CN)_6]$, (b) Effect of pH analysis, and (c) repeatability study of $MnFe_2O_4$ NPs/GP electrode. Adapted from ref. [37] Copyright @ authors

The study conducted by Pramanik et al. involved the synthesis and sensing ability of gadolinium ferrate NPs ($GdFeO_3$ NPs) toward dopamine [38]. The combustion method was used for the synthesis of $GdFeO_3$ NPs. FESEM and TEM techniques were utilized to characterize the synthesized NPs indicating their size was found to be in the range of 40-45 nm. The development of an electrochemical sensor was carried out using a mixture of $GdFeO_3$ NPs and graphite powder in a 1:4 ratio. The sensor was evaluated using CV and DPV techniques, and the results showed improved sensing capabilities with a lower detection limit (LOD) of 700 nM for the determination of dopamine. The linearity range of the sensor was between 5-10 µM, and the LOD value improved to 700 nM when the electrode was made of $GdFeO_3$/GP. The proposed sensor could detect dopamine in a range of 5 µM to 160 µM. The ability of $GdFeO_3$ NPs to sense dopamine could have potential applications in the development of diagnostic and therapeutic tools for such disorders.

Kumar et al. have synthesized cobalt ferrate nanoparticles (NPs) and characterized them using various techniques such as FESEM, energy-dispersive spectroscopy (EDS), and X-ray diffraction (XRD) [39]. The average crystalline size of the nanoparticles was reported to be around 10-12 nm with a cubic structure. The study included cyclic voltammograms of the prepared $CoFe_2O_4$ NPs/GP and bare GP for UA and GU, as well as a mixture of both substances. These cyclic voltammograms are presented in Figure 7a for UA, Figure 7b for GU,

and Figure 7c for the mixture. The results you provided suggest that both $CoFe_2O_4$ NPs /GP and bare GP underwent an irreversible oxidation process, as evidenced by the observation of oxidation peaks in the cyclic voltammograms. The peak potentials for the oxidation of $CoFe_2O_4$/GP NPs were slightly higher than those for bare GP, with UA displaying a peak potential of 676 mV and GU displaying a peak potential of 1042 mV, compared to the bare GP peak potentials of 658 mV and 1054 mV, respectively. The scan rate used in this experiment was 100 mVs^{-1}, and the cyclic voltammograms were performed over a range of potentials from 0.35 to 0.85 V for UA and 0.65 to 1.35 V for GU with a pH 5.0 buffer solution used as a supporting electrolyte. These results suggest that both $CoFe_2O_4$/GP NPs and bare GP have electrochemical activity in this potential range and can undergo oxidation reactions. The study found that the nanocomposite was able to efficiently detect these substances at low concentrations. Overall, these results provide insight into the electrochemical properties of $CoFe_2O_4$/GP NPs and bare GP and can be used to inform future studies on the use of these materials in various applications.

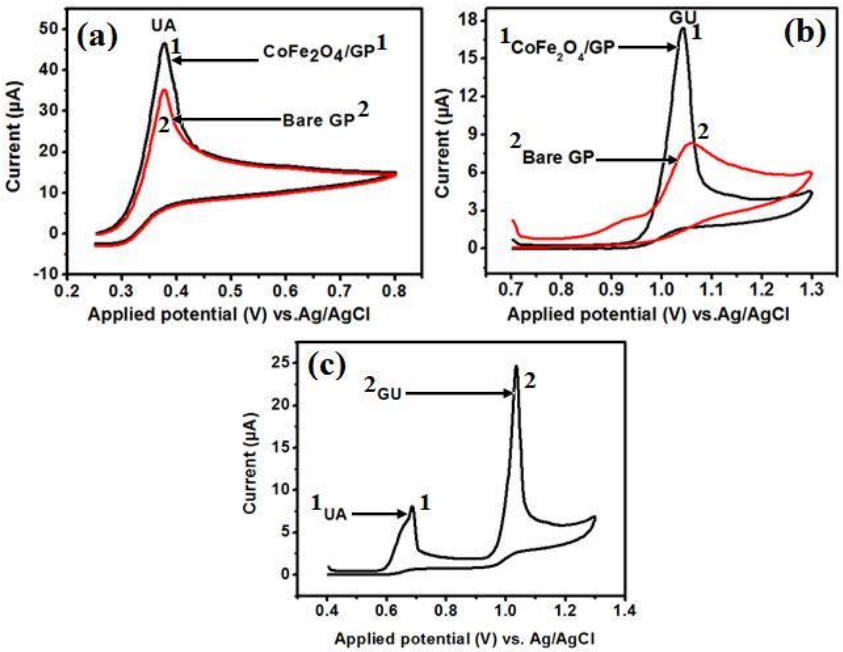

Figure 7. CV plots of 0.1 mM UA (a) at $CoFe_2O_4$ NP/GP electrodes (peak 1) and at bare GP (peak 2); 0.1 mM GU (b) at $CoFe_2O_4$/GP NP electrodes (peak 1) and at bare GP (peak 2); CV plot of 0.1 mM UA and 0.1 mM GU mixture (c) at $CoFe_2O_4$/GP NP electrodes in 0.1M phosphate buffer solution of pH 5.0 maintaining CV scan rate of 100 mVs^{-1}. Adapted from ref. [39] Copyright @ authors

Pradhan et al. have reported the development of a simple and cost-effective electrochemical sensor based on nano copper telluride (CuTe NPs) for the simultaneous detection of epinephrine (EP) and uric acid (UA) [40]. The electrochemical sensor was fabricated by

depositing the CuTe NPs onto a glassy carbon electrode (GCE) surface using a simple drop-casting method. The CuTe NPs-based sensor showed excellent electrochemical behavior towards EP and UA with high sensitivity and selectivity. The sensor exhibited linear ranges of 1-100 μM and 2-200 μM for EP and UA, respectively, with detection limits of 0.1 μM and 0.3 μM, respectively. The study found that a potential separation of 128 mV was recorded during the determination of EP and UA using DPV. Additionally, a linear relationship between EP and UA was observed at distances of 5-60 μm and 5-120 μm. The study also reported detection limits of 18 nM and 32 nM for EP and UA, respectively.

The CV data for two molecules, EP and UA suggests that the oxidation process of each molecule is irreversible on both types of electrodes. They observed an oxidation peak of EP at 594 mV on the bare GP electrode, and they found that the oxidation peak potential shifted negatively to 177 mV during successive use of the CuTe/GP electrode. Additionally, they observed a 2.87 times higher oxidation peak current of EP on the CuTe/GP electrode compared to the bare GP electrode. An oxidation peak for UA was observed at 524 mV on the CuTe/GP surface, which is 64 mV lower than the peak observed on the bare GP electrode. This shift towards a more negative potential suggests that the CuTe/GP surface promotes the oxidation of UA at a lower potential than the bare GP electrode.

In addition to the potential shift, the anodic peak current of UA on the CuTe/GP electrode was 4.89 times higher than that observed on the bare GP electrode. This increase in current may be due to an improvement in the effective surface area of the electrode, which would promote quicker electron transfer during the oxidation process. The CuTe/GP electrode may have a more porous or rough surface compared to the bare GP electrode, which would provide more sites for UA oxidation to occur. An oxidation peak for uric acid (UA) at a potential of 524 mV on a CuTe/GP (copper telluride/graphene paper) surface, which is shifted 64 mV negatively compared to a bare GP (graphene paper) electrode. This shift in peak potential could be due to the presence of the CuTe material on the electrode surface. Additionally, the anodic peak current of UA was 4.89 times higher on the CuTe/GP surface compared to the bare GP electrode. This increase in current could be attributed to the improved effective surface area of the CuTe/GP electrode, which promotes quick electron transfer.

Overall, these results suggest that the CuTe/GP electrode may be a promising material for electrochemical sensing applications, particularly for the detection of UA. The developed sensor has potential applications in the field of clinical diagnosis and monitoring of diseases related to EP and UA levels in human body fluids. The performance of CuTe nanoparticles (NPs) that have been modified with graphite paste as an electrocatalyst. The study further reports that the use of copper telluride/graphene oxide nanocomposite (CuTe/GP) was successful in detecting and determining the concentration of EP and UA in pharmaceuticals and clinical samples.

Kumar et al. synthesized neodymium ortho ferrite nanoparticles (Nd FeO_3/GP NPs) and characterized them using various analytical tools [41]. The NPs had a size range of 40-45 nm and a cubic structure. The researchers then used these NPs, along with graphite powder, to create an electrode. They used this electrode to detect paracetamol in biological fluid using CV and DPV. The prepared sensor identified paracetamol with LOD of 400 nM with a linearity range of 5uM to 120 µM in both CV (Figure 8a) and DPV (Figure 8b) with a voltage range of 0.2 to 0.8 V for CV and 0.35 to 0.6 V for DPV. At $NdFeO_3$ NPs/GP electrodes, the voltage range was adjusted between 0.2 and 0.8 V for CV and 0.35 and 0.6 V for DPV. Utilizing the $NdFeO_3$ NPs/GP electrode, a lower detection limit was discovered to be 400 nM. These voltage ranges likely refer to the voltage applied during the sensing process, as voltammetry is a type of electrochemical measurement that involves applying a voltage to a solution and measuring the resulting current. Overall, this information suggests that the developed sensor is capable of detecting paracetamol in a wide range of concentrations with good linearity and sensitivity, which could make it useful for applications such as pharmaceutical quality control or environmental monitoring.

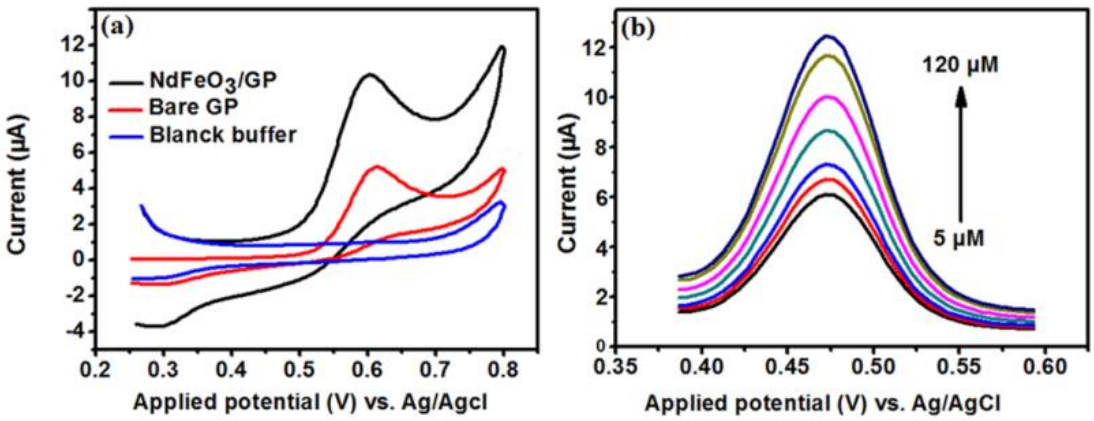

Figure 8. CV plots of (a) 0.1 mM PCM at $NdFeO_3$ NPs/GP electrodes (black), at bare GP electrode (red) and blank buffer solution (blue) (b) DPV plots from 05 µM to 120 µM PCM at np$NdFeO_3$/GP electrodes. Adapted from ref. [41] Copyright @ authors

Kumar et al. describes the synthesis of Manganese ferrite nanoparticles NPs ($MnFe_2O_4$/GP NP) using a combustion protocol, which resulted in NPs with a cubic structure and a size range of 12-14 nm [42]. The researchers used these NPs to fabricate a sensor capable of detecting UA and guanine (GU) individually and in a mixture using DPV technique. The sensor was found to have a detection limit of 400 and 450 nm for GU and UA, respectively, with a linear range of 0.5 to 120 µM for GU and 0.2 to 140 µM for UA. These findings suggest that the Manganese ferrite NPs could be a promising material for the development of sensors for the detection of UA and GU in biological and environmental samples.

Figure 9 shows the results of cyclic voltammetry (CV) and differential pulse voltammetry (DPV) studies of uric acid (UA) and guanine (GU), either individually or in a mixture. The CV plots in Figures 9a and 9b represent the oxidation behavior of UA and GU individually, respectively, while the DPV plots in Figures 9c and 9d represent the oxidation behavior of UA and GU in a mixture. Both the CV and DPV plots show an irreversible oxidation nature for UA and GU, which means that the oxidation reaction is not reversible and the resulting products cannot be converted back to the original compounds. The peak potential of the nanoparticle $MnFe_2O_4$/GP NP was found to be 673 mV and 1045 mV at bare GP, at a scan rate of 100 mVs^{-1} for CV. This suggests that the sensor is suitable for identifying UA and GU in biofluids and other forms.

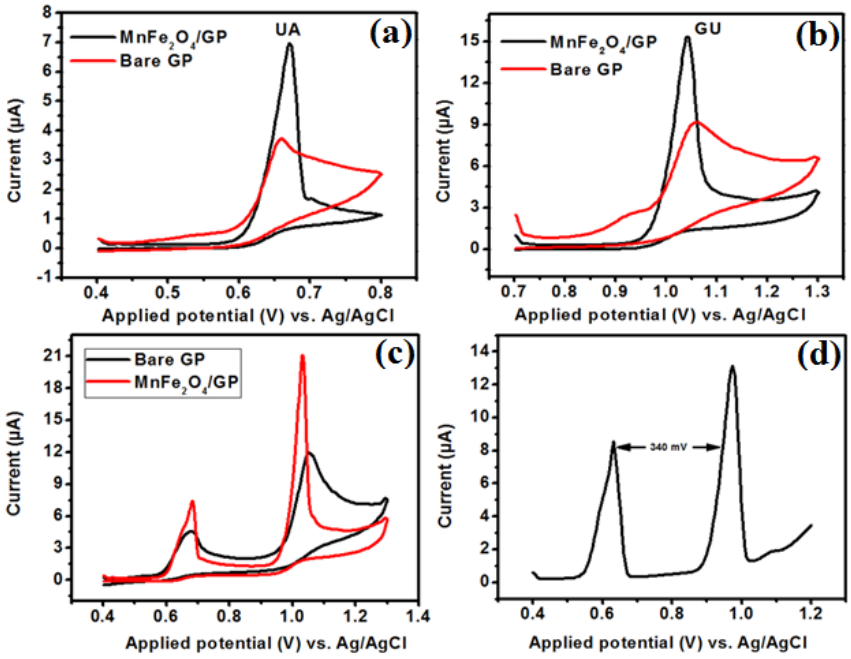

Figure 9. CV plots of 0.1 mM UA (a), 0.1 mM GU (b) at $MnFe_2O_4$ NPs/GP electrodes (black) and bare GP electrode (red), CV plot (c), and DPV plot (d) in a mixture of 0.1 mM UA and 0.1 mM GU at np$MnFe_2O_4$/GP electrode. Adapted from ref. [42]. Copyright @ authors

A research work conducted by Pradhan et al., describes the synthesis of iron telluride ($FeTe_2$) using tartrate complexes of Fe^{3+} and Te^{4+} in the presence of sodium borohydride [43]. The resulting $FeTe_2$ NPs were characterized using various analytical techniques such as XRD FESEM, and TEM. The XRD analysis confirmed the formation of orthorhombic $FeTe_2$ NPs with a diameter of 20 nm. XRD is a widely used technique for identifying crystal structures and determining the size and shape of NPs. FESEM and TEM are also commonly used for imaging and characterizing NPs at high resolution. The results obtained from CV showed that $FeTe_2$ NPs/GP were more effective in detecting DA, UA, GU, and adenine (AD) compared to bare GP of graphite paste electrodes. Furthermore, DPV analysis showed distinct oxidation

peaks corresponding to DA, UA, GU, and AD with peak potential separation of 146 mV (DA-UA), 413 mV (UA-GU), and 343 mV (GU-AD) when the electrode was dipped into a ternary biomolecule solution in buffer solution at pH 6.0. This allowed for the simultaneous identification of all four molecules.

At the bare GP electrode, anodic and cathodic peaks appeared at 407 and 241 mV, respectively, indicating a redox reaction involving DA Figure 10a. However, at the $FeTe_2$ NPs/GP electrode, a pair of redox peaks were observed at 393 and 266 mV for DA, with a peak potential separation of 127 mV, which is lower than that observed at the bare GP electrode (166 mV). This suggests that the $FeTe_2$ NPs/GP electrode is more efficient at catalyzing the redox reaction of DA than the bare GP electrode. They found that the $FeTe_2$ NPs/GP electrode had a higher peak current compared to the bare GP electrode, with a 3.5-fold increase in current. Additionally, they observed irreversible oxidation of 0.1 mM UA in CV analysis, with a negative shift of the oxidation peak potential by 21 mV for $FeTe_2$ NPs/GP compared to bare GP (Figure 10b). Furthermore, the researchers also observed an increase in the oxidation peak current of UA by 1.96 times when comparing $FeTe_2$ NPs/GP to bare GP. In another experiment using CV sliding with 0.1 mM guanine (GU), they observed irreversible oxidation peaks at 881 and 890 mV for both $FeTe_2$ NPs/GP and bare GP electrodes.

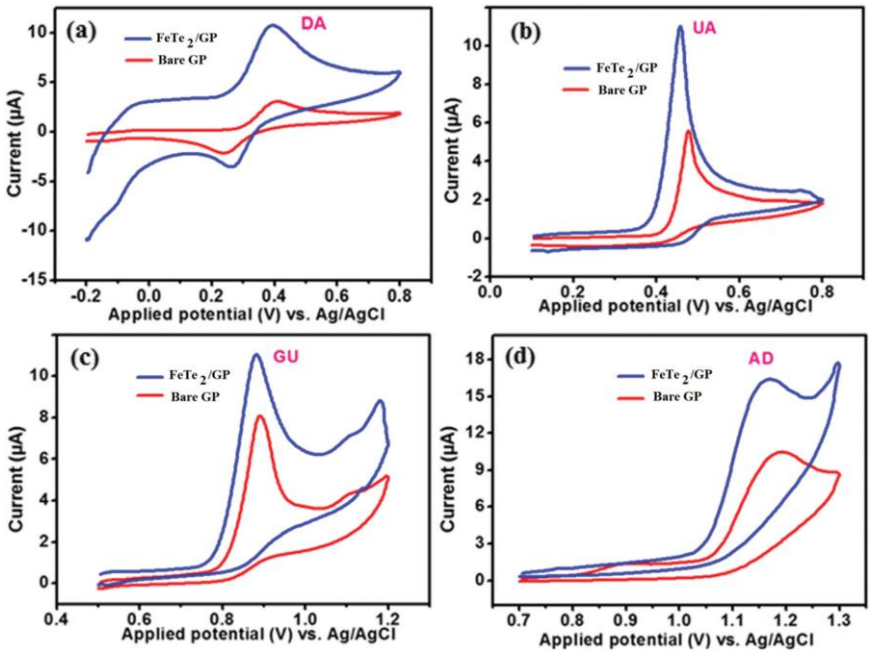

Figure 10. CV plots of 0.1 mM (a) DA, (b) UA, (c) GU, and (d) AD in 0.1 M phosphate buffer pH 6.0 at bare GP (red) and $FeTe_2$/GP (blue) electrodes. Adapted from ref. [43] Copyright @ authors

The cyclic voltammogram shown in Figure 10d indicates the oxidation behavior of AD on both bare GP and $FeTe_2$ NPs/GP electrodes. An oxidation peak is observed at 1184 mV for

bare GP, indicating the oxidation of AD on the electrode surface. A sharper oxidation peak is observed at 1164 mV for the $FeTe_2$ NPs/GP electrode, indicating that the oxidation of AD is more pronounced on the $FeTe_2$ NPs/GP surface. This suggests that $FeTe_2$ NPs/GP is a more effective electrode for the electrochemical detection of AD than bare GP. The study has shown that when compared to bare GP, the peak current for AD was 1.57 times higher. The mixture used in the study contained 0.05 mM DA, 0.1 mM UA, 0.05 mM GU, and 0.12 mM AD. The electrochemical behavior of this mixture was studied and the results have been presented in Figure 11.

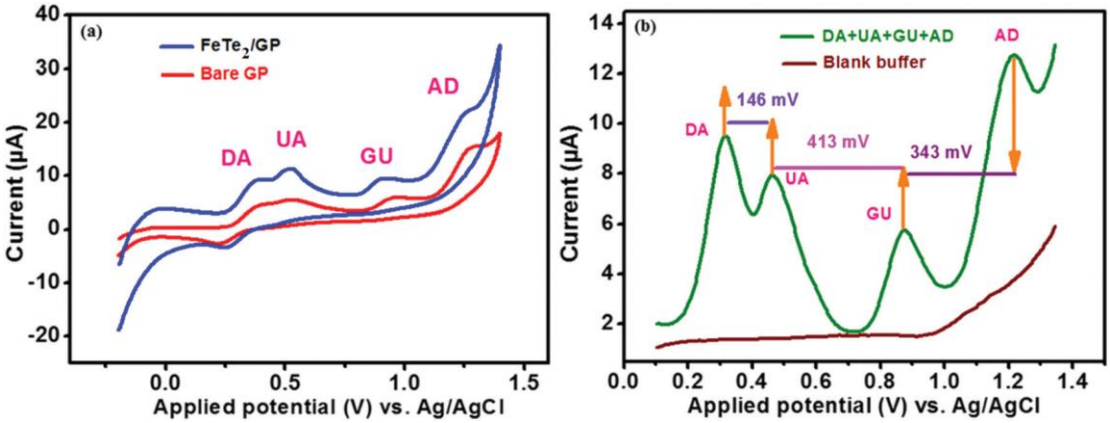

Figure 11. (a) CV plots of 0.05 mM DA, 0.1 mM UA, 0.05 mM GU, and 0.12 mM AD in the mixture at bare GP (red) and $FeTe_2$/GP (blue) electrodes and (b) DPV plots of blank buffer solution (brown line) and the mixture + 0.01 mM AD (green line). Adapted from ref. [43] Copyright @ authors

The DPV study suggested that when the mixture was added to a 0.1 M PBS solution, four well-defined peaks appeared at specific oxidation peak potential separations for different pairs of drugs (DA-UA, UA-GU, GU-AD, DA-GU, and DA-AD). The range of the potential at which the peaks appeared was 0.1 to 0.14 V, and the scan rate was 8 mVs^{-1}. DPV study was conducted on a mixture containing four drug components within a certain voltage range (0.1 to 0.14 V) and at a specific scan rate (8 mVs^{-1}). The study showed that when the mixture was added to a 0.1 M PBS (phosphate-buffered saline) solution, four well-defined oxidation peaks were observed at specific potential values (316, 462, 875, and 1218 mV), indicating the presence of the four drug components. The potential separation between the oxidation peaks for each pair of drug components (DA-UA, UA-GU, GU-AD, DA-GU, and DA-AD) was also determined, and these values were found to be 146, 413, 343, 559, and 902 mV, respectively. It is worth noting that no redox peak was observed in the blank solution, indicating that the $FeTe_2$ NPs/GP sensor used in the study was inactive in the absence of analytes. This confirms that the observed peaks were indeed due to the presence of the drug components in the mixture.

Overall, this research work provides important insights into the synthesis and characterization of $FeTe_2$ NPs, which could have potential applications in various fields such as electronics, energy storage, and catalysis. The results suggest that the oxidation of DA and UA occurred simultaneously and their peaks could not be distinguished from each other due to overlapping broad peaks. Additionally, it seems that the anodic peaks of GU and AD were not clearly visible, which could indicate slow electron transfer or fouling of the electrode due to the deposition of analytes and their oxidized products. It appeared that $FeTe_2$ NPs/GP has demonstrated impressive electrocatalytic performance in oxidizing four specific drug components. This superior performance may be attributed to the unique structural parameters of $FeTe_2$ NPs/GP, which allow for flexible valence state changes and therefore facilitate efficient electron transfer.

Kumar et al. investigated the electrocatalytic activities of $NbFeO_3$ NPs for the detection of GU and UA [44]. The researchers used $NbFeO_3$ NPs as an electrode modifier and evaluated their performance using CV and DPV techniques. The results showed that $NbFeO_3$ NPs had good electrocatalytic activity for the detection of GU and UA, both individually and in a mixture. The lower limit of detection for GU and UA was 250 and 350 nM, respectively. The linear range for the detection of GU was 0.5 to 100 μM, while for UA, it was 1 to 120 μM. The scan rate for CV and DPV was 100 and 50 mVs^{-1}, respectively.

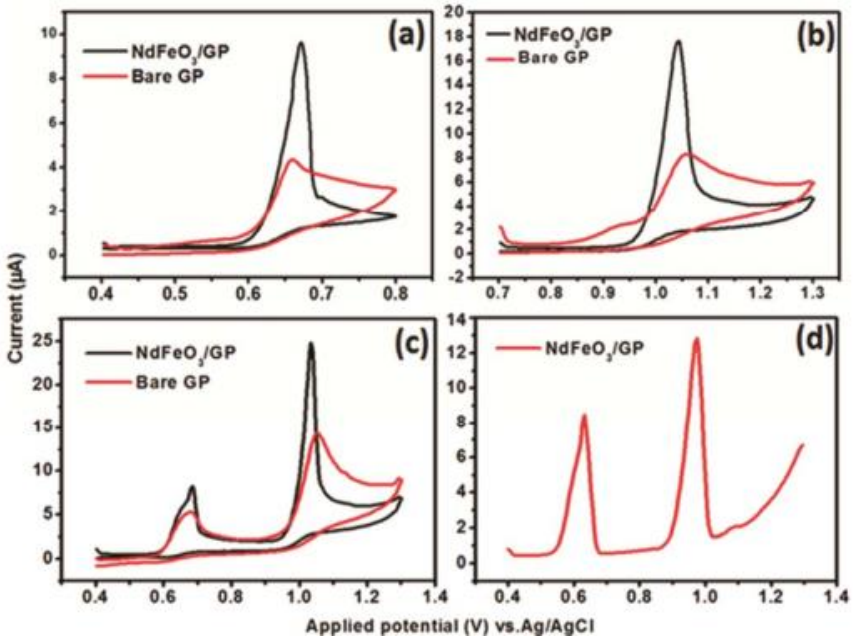

Figure 12. CV plots of (a) 0.1 mM UA at $NdFeO_3$ NPs/GP electrodes (black) and at bare GP electrode (red) (b) 0.1 mM GU at $NdFeO_3$ NPs/GP electrodes and at bare GP electrode (black) and at bare GP electrode (red) (c) CV plot in mixture of 0.1 mM UA and 0.1 mM GU of at $NdFeO_3$ NPs/GP electrodes and bare GP (red) and (d) DPV plot in mixture of 0.1 mM UA and 0.1 mM GU of at $NdFeO_3$ NPs/GP electrodes (red). Adapted from ref. [44] Copyright @ authors

Figure 12a and Figure 12b show the results of a cyclic voltammetry experiment comparing the use of bare GP electrodes and $NdFeO_3$ NPs/GP electrodes for the detection of two analytes, UA and GU. The results show that the oxidation peak potential for UA and GU were observed at 678 and 104 mV, respectively, when using the $NdFeO_3$ NPs/GP electrode, compared to 658 and 105 mV for the bare GP electrode. The study found that the peak current values for UA and GU were 9.65 and 17.17 μA, respectively, at their highest point, and at the bare cap, the values were 4.35 and 8.42 μA, respectively. To determine UA and GU individually, the cyclic voltammogram was operated within a specific potential range: from 0.35 to 0.85 V for UA and from 0.65 to 1.35 V for GU. However, during the simultaneous determination of UA and GU, the potential range was expanded to 0.35 to 1.4 V. Overall, these results suggest that cyclic voltammetry may be a useful method for detecting and quantifying UA and GU in various samples. Overall, the study suggests that $NbFeO_3$ NPs have the potential for use as an effective electrode modifier for the detection of GU and UA in various applications, such as in clinical diagnosis and environmental monitoring.

Kumar et al. have conducted a study in which they synthesized cobalt iron oxide nanoparticles ($CoFe_2O_4$ NPs) and manganese iron oxide nanoparticles ($MnFe_2O_4$ NPs) for the purpose of determining the presence of paracetamol (PCM) and DA [45]. To characterize the synthesized nanoparticles, they used XRD, FESEM, and EDS. Characterization through FESEM suggested that NPs possessed a size range of 10-12 nm and a cubic structure.

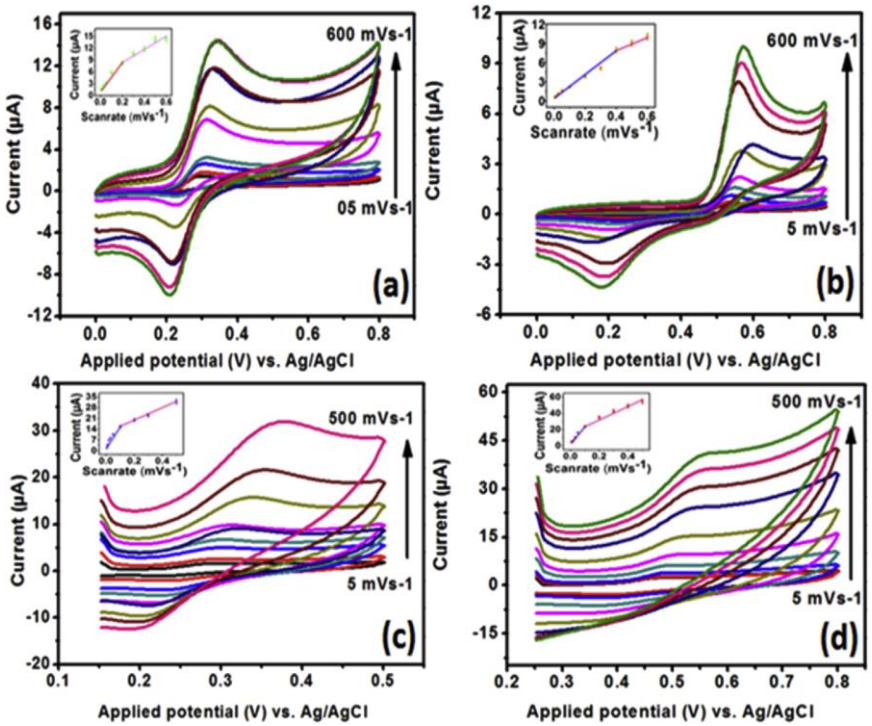

Figure 13. Scan rate of 0.1 mM (a) DA varied at $CoFe_2O_4$ NPs/GP (b) PCM varied at $CoFe_2O_4$ NPs/GP electrode (c) DA varied at $MnFe_2O_4$ NPs/GP (d) PCM varied at $MnFe_2O_4$ NPs/GP electrode. Adapted from ref. [45] Copyright @ authors

The detection limit for paracetamol and dopamine with $CoFe_2O_4$ NPs/GP was 250 nM and 350 nM, respectively. For $MnFe_2O_4$ NPs/GP, the detection limit was slightly higher at 300 nM and 400 nM for paracetamol and dopamine, respectively. The oxidation peaks for paracetamol and dopamine were well-separated in a mixture, as observed using CV and DPV with scan rates of 100 mVs^{-1} and 50 mVs^{-1}. Figure 13 shows that the oxidation process was diffusion-controlled. The pH of the buffer had an effect on the peak current of both dopamine and paracetamol, indicating that the sensor's performance could be influenced by changes in pH.

Pradhan and co-workers synthesized Lead telluride PbTe/GR nanocomposite was synthesized together by reducing graphene oxide in the presence of zinc dust [46]. XRD, FESEM, and EDX were used to characterize the resulting materials. It was suggested that adding lead telluride nanoparticles (PbTe NPs) and graphene to graphite powder enhances the electrocatalytic properties of GU and AD. A modified electrode has been developed and tested for the detection of GU and AD in spiked human urine and serum samples.

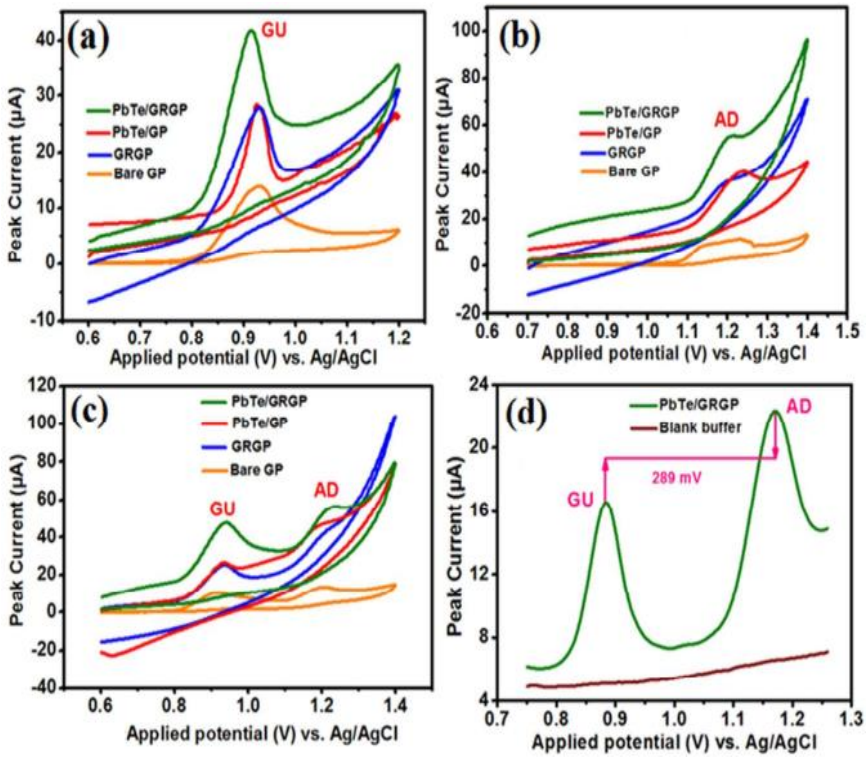

Figure 14. CV plots of (a) 0.1 mM GU (b) 0.1 mM AD at bare GP (orange), GRGP (blue), PbTe NPs/GP (red) and PbTe NPs/GRGP (green) electrodes in 0.1 M phosphate buffer (pH 5); CVs of mixtures of (c) 0.1 mM GU + 0.1 mM AD at bare GP (orange), GRGP (blue), PbTe NPs/GP (red) and PbTe NPs/GRGP (green) electrodes; DPV plot of the mixture of (d) blank buffer solution (brown line) and mixture of 0.1 mM GU + 0.1 mM AD solutions (green line) in 0.1 M phosphate buffer pH 5 at PbTe NPs/GRGP electrode. Scan rates for CV and DPV are 100 mVs^{-1}, 50 mVs^{-1} respectively. Adapted from ref. [46] Copyright @ authors

The electrode appears to have demonstrated excellent electrocatalytic performance in both CV and DPV. The results of a CV study show distinct irreversible peaks for GU and AD in contact with PbTe/GRGP (Figure 14a-c). Additionally, DPV plot (Figure 14d) displayed two well-defined peaks of GU and AD with a peak potential separation of 289 mV. The distinct peaks observed for GU and AD in the presence of PbTe NPs/GRGP suggest that the addition of these materials modifies the electrochemical behavior of the samples, potentially leading to improved electrocatalytic activity.

The electrode's performance may be attributed to the combination of both PbTe (lead telluride) and graphene materials. Graphene has a large surface area of 252 m^2/g with pore sizes ranging from 1.8 to 7.4 nm, which is beneficial for allowing biomolecules to transfer through the electrode. PbTe has an average particle size of 22 nm, which may also contribute to the electrode's performance. The probable mechanism for the electrode's performance is not explicitly stated in your statement, but it is likely that the combination of these materials allows for efficient electron transfer and a high degree of sensitivity for detecting the biomolecules of interest. The chance of π-π stacking between graphene and biomolecules is one possible mechanism by which the interaction between these two materials might be enhanced in an aqueous electrolyte.

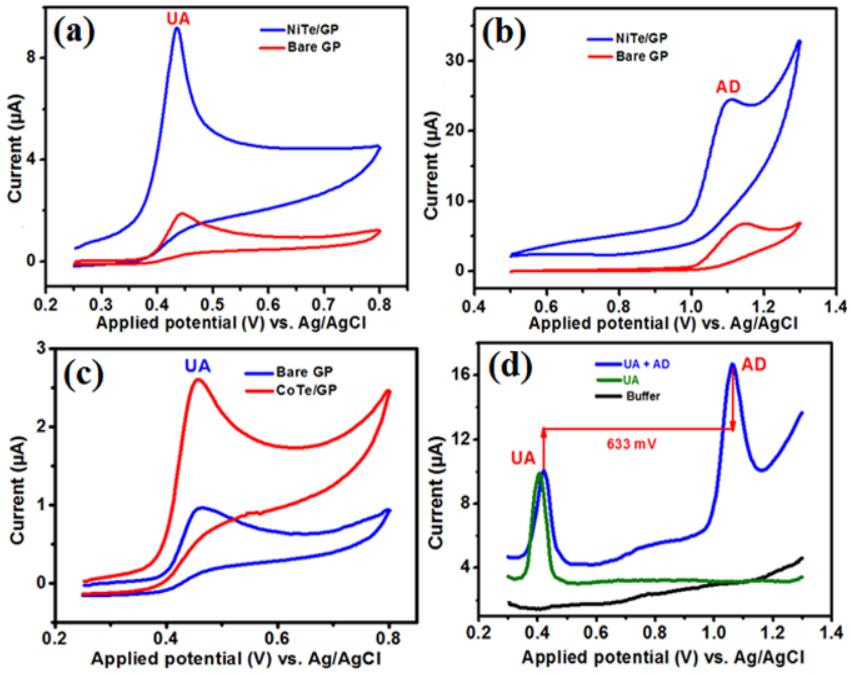

Figure 15. CV plots of (a) 0.1 mM UA, (b) 0.1 mM AD in 0.1 M phosphate buffer pH 6.0 at bare GP (red) and NiTe NPs/GP (blue) electrodes; CVs of (c) 0.05 mM UA at bare GP (blue) and CoTe NPs/GP (red) electrodes; DPV plot of (d) blank buffer solution (black line), 0.05 mM UA solution (green line) and mixture of 0.05 mM UA + 0.05 mM AD solutions (blue line) at NiTe NPs/GP electrode in 0.1 M phosphate buffer pH 6.0. For CV scan rate 100 mVs^{-1} and for DPV 50 mVs^{-1}. Adapted from ref. [22] Copyright @ authors

Pradhan et al. have successfully synthesized NiTe and CoTe nanoparticles from the tartrate complex of Ni^{2+}/Co^{2+} and Te^{4+} at room temperature using sodium borohydride reduction as the method of synthesis [47]. They have characterized the synthesized particles using various analytical tools, including XRD, FESEM, TEM, and EDX. The size distribution of the synthesized nanoparticles is reported to be 10.8 mm and 3.8 mm for NiTe and CoTe, respectively. The synthesis of NiTe and CoTe nanoparticles at room temperature using a simple reduction method is a promising approach for the production of these materials on a large scale. Specifically, the electrochemical properties were evaluated using two techniques viz. CV and DPV (Figure 15). The experiment also involved the detection of two compounds, UA and AD, using a modified graphite electrode (NiTe NPs/GP). The detection of UA and AD was accomplished using DPV, and the results show that the lower detection limit for UA was 95 nM in a mixture, with a linear response range of 3-200 μM. For AD, the lower detection limit was 206 nM in a mixture, with a linear response range of 3-50 μM.

The results suggest that a NiTe NPs/GP electrode has superior sensitivity compared to a bare GP electrode in detecting UA. The CV of UA for the NiTe NPs/GP electrode showed an irreversible oxidation character, with a negative shifting of oxidation peak potential of 10 mV compared to the bare GP electrode. The oxidation peak current value for the NiTe NPs/GP electrode was also 5.13 times higher than that of the bare GP electrode (Figure 15a). In addition, the electrode also displayed good reversibility and significant electrocatalytic performance, as evidenced by the sharp anodic peak appearing at 1099 mV for AD compared to 1130 mV for the bare GP electrode (Figure 15b). The oxidation peak current value for the NiTe NPs/GP electrode was also 3.8-fold higher than that of the bare GP electrode, suggesting that the NiTe NPs/GP electrode has excellent electrocatalytic properties.

Figure 15a shows the CV of UA for NiTe NPs/GP and bare GP electrodes, revealing that both electrodes displayed irreversible oxidation. However, the peak potential of NiTe NPs/GP shifted negatively by 10 mV compared to bare GP, indicating a difference in their redox behavior. Furthermore, NiTe NPs/GP had 5.13 times more oxidation peak current than bare GP, suggesting that the NiTe NPs/GP electrode was more efficient at detecting UA.

Figure 15c apparently shows the redox nature of CoTe NPs/GP. It reveals that the oxidation peak current was 2.69 and 1.02 for UA, which suggests that CoTe NPs/GP is excellent at detecting UA individually. A broad oxidation peak of AD at 1130 mV on bare GP was observed, which indicates that AD molecules underwent oxidation at a relatively broad range of voltages. On the other hand, on NiTe NPs/GP, a sharp anodic peak of AD appeared at a lower voltage of 1099 mV. An anodic peak refers to a positive peak in the electrochemical response, which suggests that AD underwent oxidation at this voltage. The sharpness of the peak may indicate a more well-defined electrochemical behavior of AD molecules on the NiTe NPs/GP electrode, possibly due to the presence of NiTe (nickel telluride) on the surface of the electrode.

The results showed that the oxidation peak current for NiTe NPs/GP was 3.8 times higher than that for bare GP, indicating better reversibility and electrocatalytic activity towards UA and AD (Figure 15b). This work suggests that this could be due to the high absorptivity and faster electron transfer ability of NiTe material. In contrast, the oxidation peak current for CoTe NPs/GP was lower, indicating slower electron transfer and a lack of ability for simultaneous detection of UA and AD. The authors propose that this is likely due to the slow electron transfer at CoTe NPs/GP, which makes it less efficient as an electrocatalyst for these analytes.

In the study, the researchers investigated the redox behavior of UA (uric acid) towards CoTe NPs/GP (cobalt telluride/graphene paper) and represented their findings in Figure 15c. The results showed that the peak current value of UA for CoTe NPs/GP was 2.69 μA, while for bare GP, it was 1.02 μA. This indicated that CoTe NPs/GP was more effective than bare GP in detecting UA. To achieve better resolution than CV, the researchers used DPV (to detect UA and AD) simultaneously. Controlled DPV was also performed to evaluate the specificity of oxidation peaks of biomolecules, as shown in Figure 15d. The results suggest that the CoTe NPs/GP electrode is a promising candidate for the detection of UA, but may not be suitable for detecting multiple analytes simultaneously. The study also highlights the potential benefits of using modified electrodes, such as NiTe NPs/GP, for improving the sensitivity and selectivity of electrochemical sensors.

4. CONCLUSION AND FUTURE PERSPECTIVES

The growing interest in electrochemical techniques and the development of more advanced methods have made it possible to conduct precise and accurate quantitative analyses of pharmaceuticals. Electrochemical sensors have gained a lot of attention in recent years for their high sensitivity, selectivity, and accuracy in detecting various chemical compounds. Electrochemical sensors have proven to be a reliable and effective means of detecting a wide range of substances, including gases, liquids, and biological molecules. Nanocomposites have emerged as a promising material for developing electrochemical sensors due to their unique physical and chemical properties, such as high surface area, enhanced catalytic activity, and excellent electrical conductivity.

Nanocomposite-based electrochemical sensors discussed herein show great promise for the detection of biologically important compounds such as dopamine, guanine, adenine, and uric acid. These sensors offer advantages such as high sensitivity, selectivity, and stability, as well as low cost and ease of fabrication. However, further research is needed to optimize the performance of these sensors and to explore their potential in various applications.

One of the key advantages of electrochemical sensors is their ability to detect minute quantities of analytes without causing significant damage or altering the sample. This is particularly important in medical diagnostics, where the accuracy and precision of the test results are crucial. In the years to come, electrochemical sensors are expected to play an

increasingly important role in medical diagnostics, as they offer several advantages over traditional diagnostic methods, such as faster results, lower costs, and greater accuracy. With further advancements in sensing technology, biosensors will likely become even more sensitive, specific, and versatile, paving the way for new applications in healthcare and beyond.

Acknowledgments

The author is grateful to the Department of Chemistry, GLA University, Mathura, India for all kinds of support in this study.

Conflict of interest

The author declares no conflict of interest.

REFERENCES

[1] S.W. Baran, P.C. Brown, A.R. Baudy, S.C. Fitzpatrick, C. Frantz, A. Fullerton, J. Gan, R.N. Hardwick, K.M. Hillgren, A.K. Kopec, and J.L. Liras, ALTEX-Alternatives to Animal Experimentation 39 (2022) 297.
[2] V.K. Vashistha, Asian J. Organic Chem. 11 (2022) 202200544.
[3] V.K. Vashistha, S. Sethi, I. Tyagi, and D.K. Das, Asian Biomedicine 16 (2022) 55.
[4] F. Meissner, J. Geddes-McAlister, M. Mann, and M. Bantscheff, Nature Reviews Drug Discovery 21 (2022) 637.
[5] T.Y. Hou, C. Chiang-Ni, and S.H. Teng, J. Food Drug Anal. 27 (2019) 404.
[6] V.K. Vashistha, N. Verma, R. Kumar, I. Tyagi, A. Gaur, and R. Bala, Chirality 34 (2022) 1044.
[7] V.K. Vashistha, Detection and remediation of chiral pharmaceuticals from wastewater: A review. Chirality 34 (2022) 833.
[8] S. Alwera, V. Alwera, and S. Sehlangia, Biomed. Chromatography 34 (2020) e4943.
[9] V.K. Vashistha, Current Anal. Chem. 18 (2022) 440.
[10] D. Gupta, S. Bhardwaj, S. Sethi, S. Pramanik, D.K. Das, R. Kumar, P.P. Singh, and V.K. Vashistha, Spectrochim. Acta Part A (2022) 120819.
[11] V.K. Vashistha, R. Bala, and R. VSR Pullabhotla, J. Taibah University for Sci. 17 (2023) 2206363.
[12] M. Donegan, J.M. Nguyen, and M. Gilar, J. Chromatography A 1666 (2022) 462860.
[13] A. Guironnet, C. Sanchez-Cid, T.M. Vogel, L. Wiest, and E. Vulliet, J. Chromatography A 1651 (2021) 462133.
[14] M.J. Gunsch, E.L. Schwalm, C.M. Ouimet, H.M. Halsey, S.E. Hamilton, F. Bernardoni, and J. Jo, J. Pharm. Biomed. Anal. 213 (2023) 114684.

[15] S. Salido-Fortuna, M. Castro-Puyana, and M.L. Marina, J. Chromatography A 1626 (2020) 461383.
[16] B. Pasquini, R. Gotti, M. Villar-Navarro, M. Douša, L. Renai, M. Del Bubba, S. Orlandini, and S. Furlanetto, J. Pharm. Biomed. Anal. 202 (2022) 114163.
[17] F. Akter, and S.A. Shamsi, J. Chromatography A 1617 (2020) 460835.
[18] C. Filep, M. Szigeti, R. Farsang, M. Haberger, D. Reusch, and A. Guttman, Anal. Chim. Acta 1166 (2021) 338492.
[19] H.S. Elbordiny, S.M. Elonsy, H.G. Daabees, and T.S. Belal, Sustainable Chem. Pharm. 27 (2022) 100684.
[20] W. Nabgan, M. Saeed, A.A. Jalil, B. Nabgan, Y. Gambo, M.W. Ali, M. Ikram, A.A. Fauzi, A.H.K. Owgi, I. Hussain, and A.A. Thahe, Environ. Res. 210 (2022) 112975.
[21] M. Ehsani, J. Soleymani, P. Mohammadalizadeh, M. Hasanzadeh, A. Jouyban, M. Khoubnasabjafari, and Y. Vaez-Gharamaleki, Microchem. J. 165 (2021) 106101.
[22] V. Naresh, and N. Lee, Sensors 21 (2021) 1109.
[23] J.A. Buledi, Z.U.H. Shah, A. Mallah, and A.R. Solangi, Current Anal. Chem. 18 (2022) 102.
[24] T. Tite, E.A. Chiticaru, J.S. Burns, and M. Ioniţă, J. Nanobiotechnol. 17 (2019) 1.
[25] J. Baranwal, B. Barse, G. Gatto, G. Broncova, and A. Kumar, Chemosensors 10 (2022) 363.
[26] N. Chaudhary, and M. Khanuja, Electrochemistry—Concepts and methodologies. In Electrochemical Sensors (2022) (pp. 31-50), Woodhead Publishing.
[27] S. Amemiya (2007) Potentiometric ion-selective electrodes. In Handbook of electrochemistry (pp. 261-294). Elsevier.
[28] F. Scholz, ChemTexts, 1 (2015) 17.
[29] C. Sandford, M.A. Edwards, K.J. Klunder, D.P. Hickey, M. Li, K. Barman, M.S. Sigman, H.S. White, and S.D. Minteer, Chem. Sci. 10 (2019) 6404.
[30] P.R. Haddad, Chapter 10, Electrochemical detection (amperometry, voltammetry, and coulometry). J. Chromatogr. Lib. 46 (1990) 291.
[31] H.S. Magar, R.Y. Hassan, and A. Mulchandani, Sensors 21 (2021) 6578.
[32] J.M. Pingarrón, J. Labuda, J. Barek, C.M. Brett, M.F. Camões, M. Fojta, and D.B. Hibbert, Terminology of electrochemical methods of analysis (IUPAC Recommendations 2019), Pure and Applied Chem. 92 (2020) 641.
[33] P.A. Fritz, B. Bera, J. Van Den Berg, I. Visser, J.M. Kleijn, R.M. Boom, and C.G.P.H. Schroën, Langmuir 37 (2021) 6549.
[34] A. Varma, A.S. Mukasyan, A.S. Rogachev, and K.V. Manukyan, 116 (2016) 14493.
[35] A.S. Mukasyan, A.S. Rogachev, and S.T. Aruna, Advanced Powder Technology 26 (2015) 954.

[36] S. Pramanik, P. Karmakar, and D.K. Das, Biointerface Res. Applied Chem. 13 (2023) 134.
[37] Y. Kumar, P.P. Singh, J.K. Ajish, and M. Kumar, Res. J. Chem. Environ. 26 (2022).
[38] S. Pramanik, Y. Kumar, P. Karmakar, and D.K. Das, Nano Life 11 (2021) 2150002.
[39] Y. Kumar, V. Sharma, V.K. Vashistha, R.V. Pullabhotla, and D.K. Das, Chem. 15 (2021) 520.
[40] S. Pradhan, M.B. Banerjee, S. Biswas, N.A. Hamizi, D.K. Das, R. Bhar, R. Bandyopadhyay, and P. Pramanik, Electroanalysis 33 (2021) 383.
[41] Y. Kumar, V.K. Vashistha, and D.K. Das, Lett. Applied NanoBioSci. 9 (2020) 866.
[42] Y. Kumar, V.K. Vashistha, V. Sharma, R. Patil, and D.K. Das, Anal. and Bioanal. Electrochem. 12 (2020) 653.
[43] S. Pradhan, S. Pramanik, D.K. Das, R. Bhar, R. Bandyopadhyay, P. Millner, and P. Pramanik, New J. Chem. 43 (2019) 10590.
[44] Y. Kumar, P.P Singh, P. Pramanik, and D. Das, J. Sci. Industrial Res. 78 (2019) 177.
[45] Y. Kumar, P. Pramanik, and D.K. Das, Heliyon 5 (2019) e02031.
[46] S. Pradhan, S. Biswas, D.K. Das, R. Bhar, R. Bandyopadhyay, and P. Pramanik, New J. Chem. 42 (2018) 564.
[47] S. Pradhan, R. Das, S. Biswas, D.K. Das, R. Bhar, R. Bandyopadhyay, and P. Pramanik, Electrochim. Acta 238 (2017) 185.